

Multimodality imaging evaluation of a primary cardiac lymphoma



Paolo Ciancarella ^{a,*}, Armando Fusco ^a, Daniele Citraro ^a, Massimiliano Sperandio ^a, Roberto Floris ^a

^a Department of Diagnostic Imaging and Interventional Radiology, Molecular Imaging and Radiotherapy, University of Tor Vergata, Rome

^a Italy

Primary cardiac lymphoma is a rare form of non-Hodgkin lymphoma that involves the heart with extension to pericardium and great vessels. Prognosis is poor in the absence of a prompt diagnosis and adequate therapy. Differential diagnosis includes malignant neoplasms such as angiosarcoma or metastatic carcinoma and melanoma. Clinical manifestations may be heterogeneous. Multimodality imaging work-up represents the best method for tumor detection and evaluation of its size and extension: echocardiography, computed tomography, magnetic resonance imaging, and nuclear imaging are the best imaging tools. Definitive diagnosis is achieved with cytological and histological evaluation. We report the case of a 76-year-old woman admitted to our emergency department with symptoms of congestive heart failure. Multimodality imaging work-up showed a mediastinal bulky tumor involving heart and pericardium. Pathology revealed a large B-cell primary cardiac lymphoma.

© 2016 The Authors. Production and hosting by Elsevier B.V. on behalf of King Saud University. This is an open access article under the CC BY-NC-ND license (<http://creativecommons.org/licenses/by-nc-nd/4.0/>).

Keywords: Cardiovascular imaging, CT, MRI, Primary cardiac lymphoma, PETCT

Case report

A 76-year-old woman with no history of cardiac disease was admitted to our emergency department because of symptoms of dyspnea at rest, and episodes of chest pain occurred in recent weeks. The patient had no complaints of fever, sweat, or weight loss (B symptoms). She was

tachycardic and tachypneic with blood pressure of 90/60 mmHg. Blood count, liver, and renal functions and coagulation profile test were all within normal limits. Written consent was obtained from the patient for each of the subsequent examinations.

Chest X-ray showed an enlarged heart with loss of normal right cardiac silhouette in absence of signs of pulmonary edema (Fig. 1). Transthoracic

Disclosure: Authors have nothing to disclose with regard to commercial support.

Received 20 May 2016; revised 26 August 2016; accepted 3 September 2016.

Available online 20 September 2016

* Corresponding author at: Department of Diagnostic Imaging and Interventional Radiology, Molecular Imaging and Radiotherapy, University of Tor Vergata, Viale Oxford, 81 00133 Rome, Italy.
E-mail address: paolociancarella@hotmail.it (P. Ciancarella).



P.O. Box 2925 Riyadh – 11461KSA
Tel: +966 1 2520088 ext 40151
Fax: +966 1 2520718
Email: sha@sha.org.sa
URL: www.sha.org.sa



1016–7315 © 2016 The Authors. Production and hosting by Elsevier B.V. on behalf of King Saud University. This is an open access article under the CC BY-NC-ND license (<http://creativecommons.org/licenses/by-nc-nd/4.0/>).

Peer review under responsibility of King Saud University.
URL: www.ksu.edu.sa
<http://dx.doi.org/10.1016/j.jsha.2016.09.001>



Production and hosting by Elsevier



Figure 1. (A) Posterior–anterior and (B) and latero–lateral chest X-ray projections showing the enlargement of the heart with loss of right cardiac silhouette and no signs of pulmonary edema.

echocardiography revealed pericardial effusion with an ill-defined hypoechoic mass infiltrating the free wall of the right heart chambers.

Contrast-enhanced chest computed tomography (CT) excluded other causes of acute chest pain such as aortic dissection and pulmonary embolism. The scan revealed a large infiltrating mass localized in the pericardial space, contiguous to the anterior myocardial walls of right atrium and ventricle. The bulk showed extension to the atriocaval junction, superior vena cava, and through the atrioventricular groove involving the base of the heart. Furthermore, there was evidence of pericardial effusion that reached the upper recesses. Relative homogeneous enhancement of the mass was observed after intravenous contrast material administration (Fig. 2).

Pericardiocentesis with drainage was performed, with a substantial improvement of patient clinical and hemodynamic conditions. A large amount of mixed serous–hemorrhagic fluid was collected and used for cytologic examinations: analysis of pericardial fluid did not allow a definitive diagnosis. A subsequent second contrast-enhanced CT scan was made; unfortunately electrocardiography (ECG) synchronization was not available for this examination (Fig. 3).

During hospitalization, contrast-enhanced cardiac magnetic resonance imaging (MRI) was performed to evaluate motion relationship between the mass and the right heart chambers, the right atrioventricular wall involvement, the functional impairment of the right ventricle, the left ventricular function, and for a better tissue characterization of the mass. In order to study the possible alterations of cardiac wall kinetics, myocardium

thickness, and parietal contractility caused by the neoplasia, retrospective ECG-triggered balanced turbo field echo (steady state free precession) sequences were performed. The sequences were oriented on short and long axis (atrium–ventricular and 4-chamber view), with the following parameters: repetition time 3.8 ms; echo time 1.8 ms; flip angle 70°; matrix scan 256 × 256; thickness 8 mm; gap 0 mm; 20 cardiac phases/cycle; and retrospective synchronization.

The examination showed impaired motion of lateral and inferior right ventricular wall, right atrium compression, and basal invasion of right atrium (Figs. 4 and 5, Cine 1–3).

Precontrast black blood turbo spin echo T1, T2, and fat saturation T2 (STIR) on the axial plane were performed (Fig. 6); triggered short axis and four-chamber view T2 black blood sequences were performed to avoid heart motion artifacts (technical parameters were: repetition time 1333 ms; echo time 100 ms; TI 290 ms; echo planar imaging factor 1; turbo factor 33; matrix scan 512 × 512; slice thickness 8 mm; gap 0.8 mm; prospective diastolic synchronization; and 1 slice per breath-hold) and four-chamber T1 high-resolution isotropic volume excitation and turbo spin echo T1 sequence postinjection of 17 mL gadolinium–diethylenetriamine pentacetate (0.5 mmol) were performed on the axial plane. The postgadolinium sequences showed hyperintensity of the signal within the mass after 140 seconds (Fig. 7).

Whole body fludeoxyglucose–positron emission tomography/CT scan was used for the staging procedure: the mass showed elevated fludeoxyglucose accumulation with high Standardized Uptake Values suggesting a malignant nature of the neoplasm with high glucose

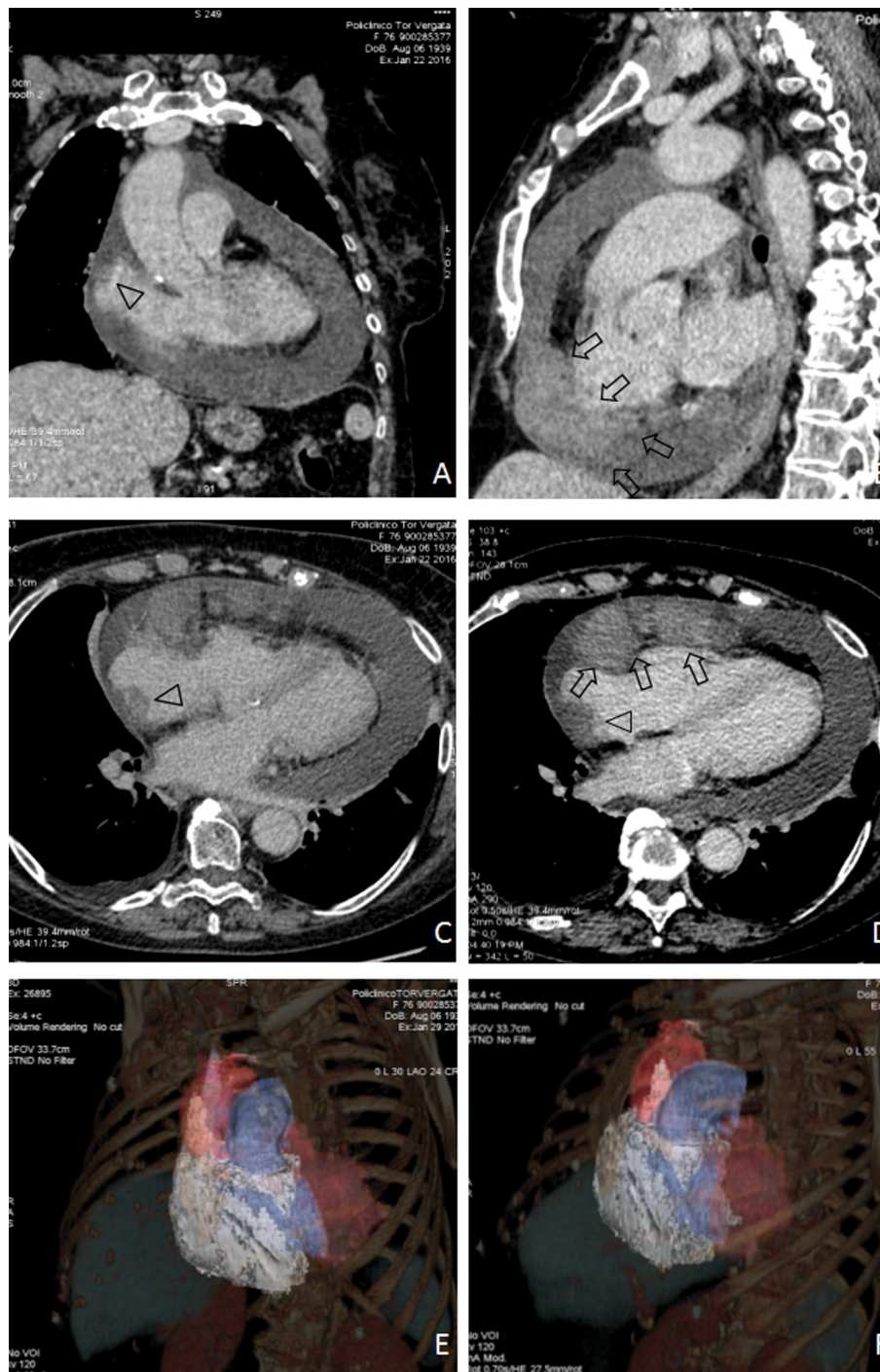


Figure 2. Contrast-enhanced chest computed tomography scan; (A) coronal, (B) sagittal, and (C, D) axial views showing a large infiltrating mass localized in the pericardial space, contiguous to the right chambers, involving also the base of the heart (empty arrows) and with extension to the atriocaval junction and superior vena cava (arrowheads). There was also evidence of pericardial effusion that reached the upper recesses. (E, F) Volume rendering reconstructions showing the mass (white color) and relationships with the above mentioned cardiac structures.

metabolism (Fig. 8). The examination showed no other localizations of disease (Fig. 9).

The patient finally underwent an open chest biopsy through median sternotomy: detailed histological examination of the tumor revealed that it was a diffuse large B-cell lymphoma. The

patient then started combined treatment with systemic chemotherapy and rituximab, an anti-CD 20 monoclonal antibody (R-CHOP protocol); at present, she is alive, asymptomatic, and keeps receiving the treatment in the absence of signs of progression of the disease.

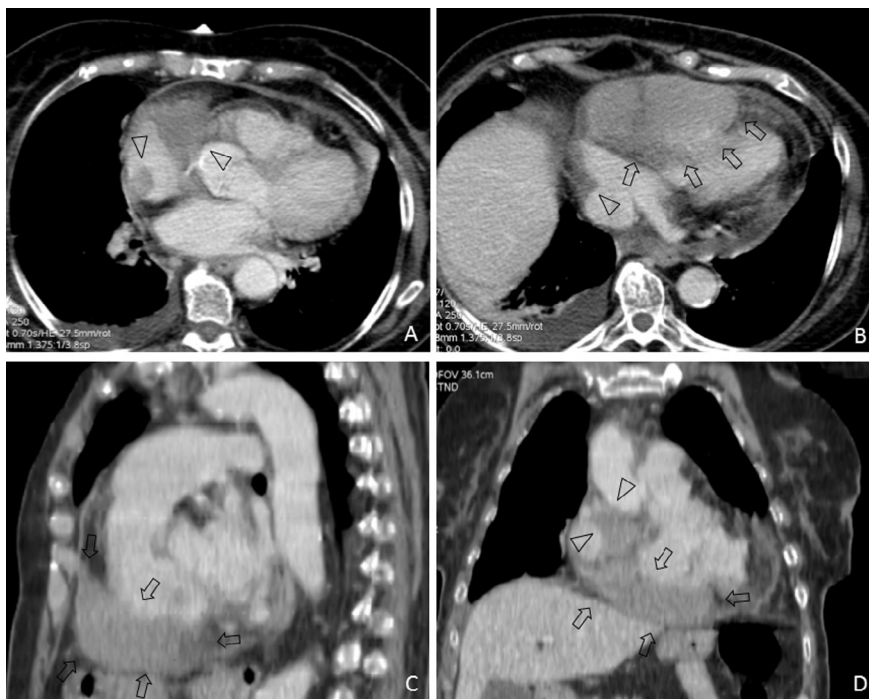


Figure 3. After pericardiocentesis, a contrast-enhanced computed tomography scan was performed with an improved visualization of the mass (arrows) and its extension (arrowheads).

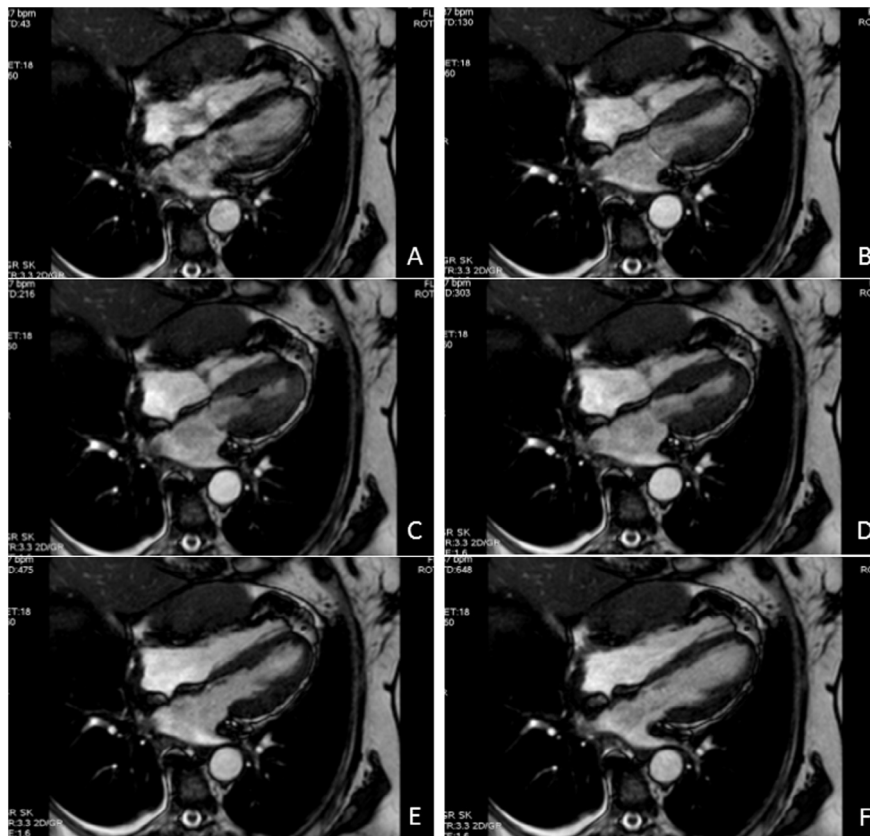


Figure 4. (A–F) Magnetic resonance imaging with retrospective electrocardiography-triggered balanced-turbo field echo (steady-state free precession) sequence showing impaired diastolic dilatation of lateral and inferior right ventricular wall, right atrium compression, and basal invasion of right atrium; despite not being hemodynamically significant, this finding is particularly evident during diastolic phase.

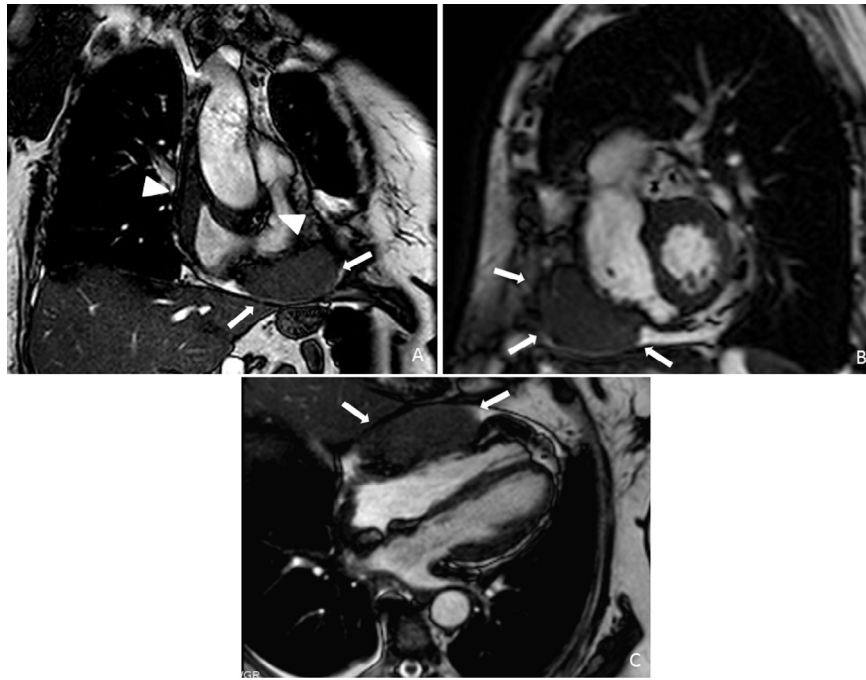


Figure 5. (A) Right ventricular long axis two-chamber view with partial identification of the pulmonary outflow, (B) short axis view, and (C) four-chamber axial view with evidence of neoplasm involving great vessels and right atrium (arrowheads), and inferior right ventricular wall (arrows); see also Cine 1–3 for dynamic view of these findings.

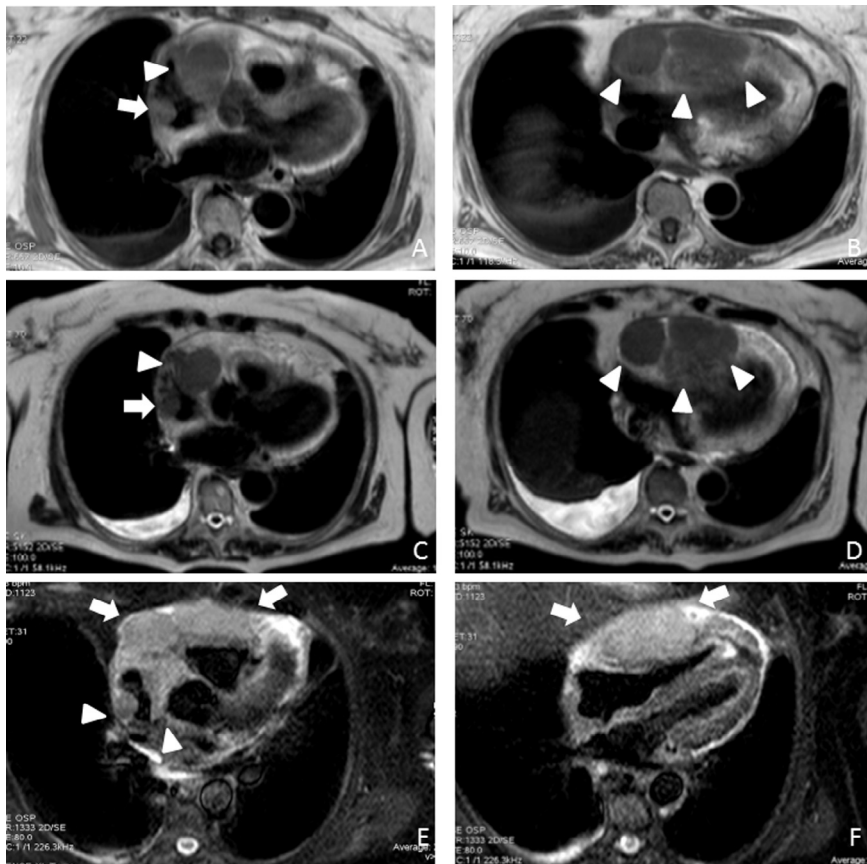


Figure 6. (A, B) Magnetic resonance imaging precontrast black blood turbo spin echo T1; (C, D) T2; and (E, F), fat saturation T2 (STIR) showing the mass (arrowheads) and its extension to vessels (solid arrow) and within cardiac structures.

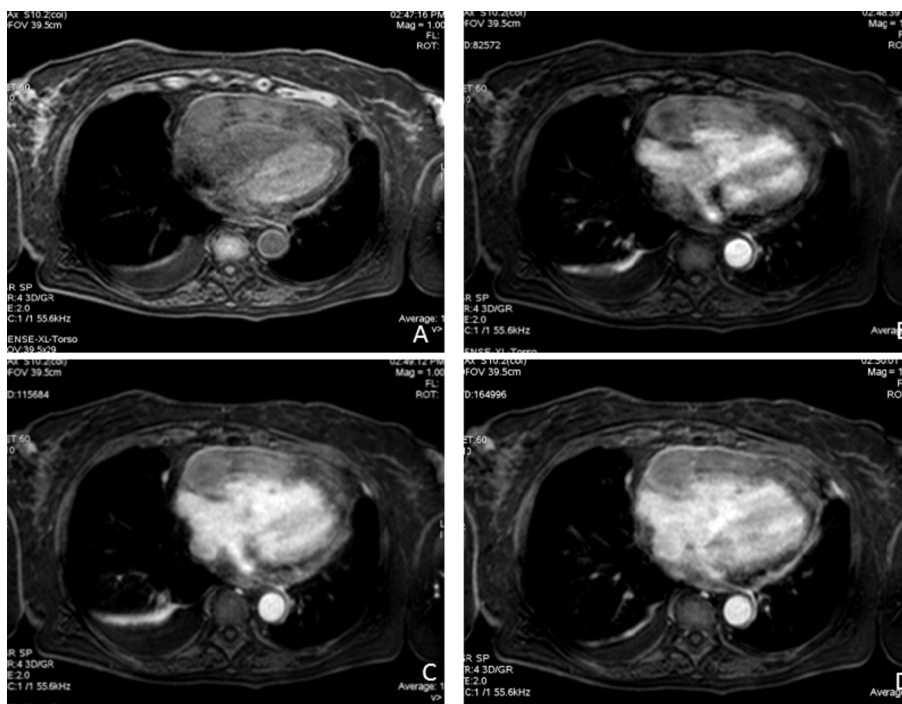


Figure 7. (A–D) Magnetic resonance imaging four chamber T1 high-resolution isotropic volume excitation and turbo spin echo T1 sequence post-17 mL of gadolinium–diethylenetriaminepentacetate (0.5 mmol) injection. The postgadolinium sequences show mild enhancement within the mass after 140 seconds.

Discussion

Primary lymphoma of the heart is extremely rare: it represents only 1.3% of all primary cardiac tumors and 0.5% of all extranodal lymphomas [1,2]. By contrast, secondary involvement of the heart is more common, with nearly 30% of patients with disseminated non-Hodgkin lymphoma demonstrating cardiac involvement on autopsy [3]. However, whether the lymphoma is primary or secondary, there are no differences in imaging findings between the two conditions. There are no unified criteria about the definition of primary cardiac lymphoma (PCL): generally, PCL involves the pericardial space and myocardium without any other extracardiac localizations. PCL usually occurs in the adult population with a male-to-female ratio of 2:1 [4]. PCL is far more common in patients with immunodeficiency state associated with human immunodeficiency virus or in transplant recipients. The majority (over 70% of cases described) of PCLs are clinically aggressive diffuse large B cell lymphomas; rare T cell lymphomas have been reported [4–6].

Cardiac tumors are called the great mimickers because they can present with various clinical presentations. There are no pathognomonic clinical features of PCL and the symptoms are often non-specific and reflects the localization and extension

of the bulk in the heart and the mediastinum: dyspnea, chest pain, congestive heart failure, different patterns of disturbance of hemodynamics due to involvement of heart and great vessels, cardiac tamponade due to pericardial effusion or hemopericardium, superior vena cava syndrome, arrhythmias such as atrial-ventricular blocks, thrombosis, and embolism.

Integrated imaging approach is mandatory because PCL demonstrates variable radiological features: initial diagnosis includes chest radiography, ECG (both transthoracic echocardiogram and transesophageal echocardiogram), CT, MRI, and nuclear imaging. ECG represents a quick noninvasive approach to patients with dyspnea and cardiac enlargement chest radiography: lymphomatous involvement of the heart appears as hypoechoic nodular myocardial mass or ill-defined bulk often infiltrating right cardiac chambers, associated with pericardial effusion.

Although initial diagnosis of a cardiac mass could be suspected with echocardiography in many cases, the technical limitations of ultrasound impose the use of cross-sectional imaging: CT and MRI represent the subsequent steps for further characterization of the tumor and its extension [7,8].

On CT imaging, PCL appears as a soft-tissue mass iso-hypoattenuating relative to the myocar-

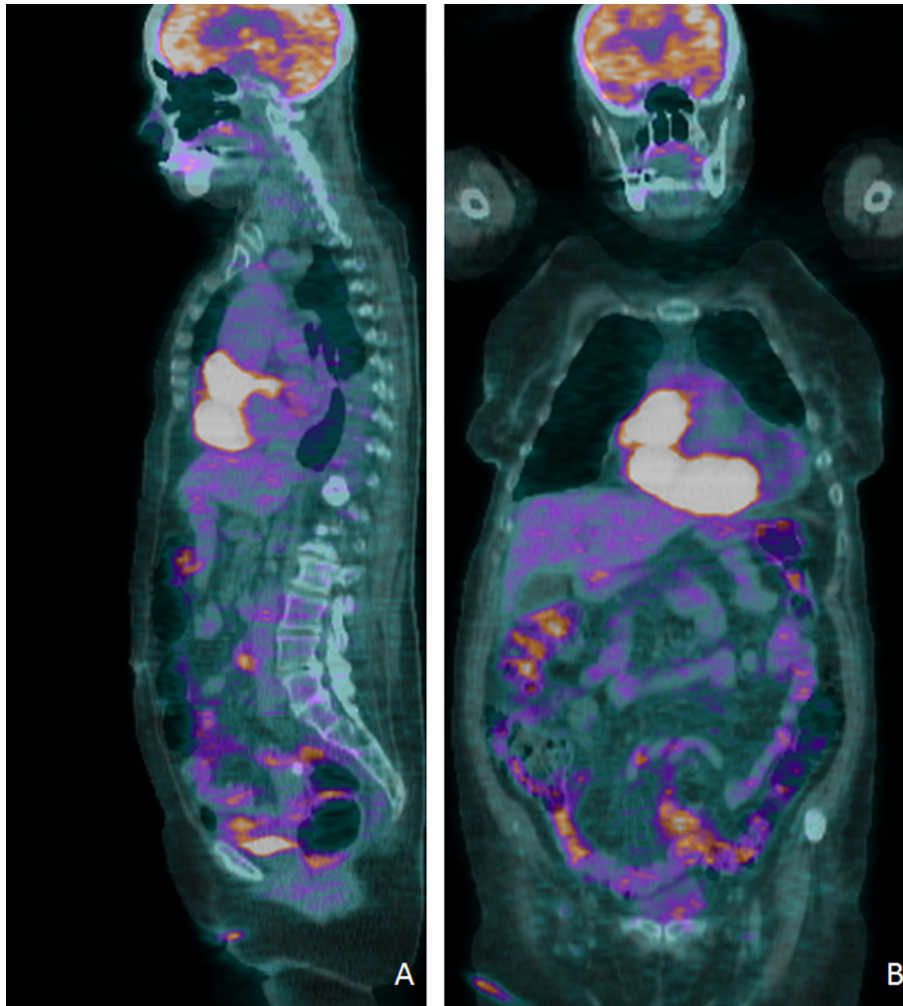


Figure 8. (A, B) Positron emission tomography–computed tomography scans; axial view showing elevated 18-fluorodeoxyglucose accumulation within the mass with high Standardized Uptake Values suggesting a malignant nature of the neoplasm with high glucose metabolism.

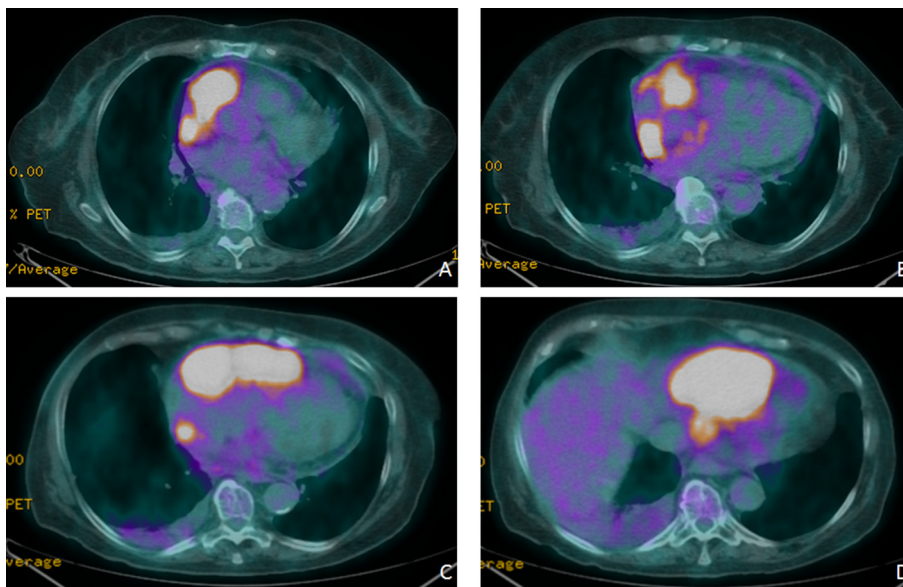


Figure 9. (A–D) Positron emission tomography–computed tomography scan; sagittal and coronal views showing no extracardiac localizations of the disease.

dium, extending along the epicardial surface wrapping and infiltrating myocardium, pericardium, great vessels, and coronary arteries. It demonstrates heterogeneous enhancement after intravenous contrast material administration. When possible, ECG-gated cardiac computed tomography, as reported in the 2010 guidelines, is an appropriate tool to evaluate intra- and extracardiac structures; it also represents the best way to evaluate the coronary artery and vein systems [7].

MRI is the best choice to depict accurately the extent myocardial and pericardial infiltration. According to the 2010 guidelines, MRI may be used for evaluation of cardiac masses, extracardiac structures, and involvement and characterization of masses in the differentiation of tumors from intracavitary mural thrombi. It also helps in discriminating between benign versus malignant cardiac masses emphasizing infiltration, invasion, and other signs of metastasis [8].

PCL can be hypointense on T1-weighted imaging and hyperintense on T2-weighted imaging, but it can demonstrate heterogeneous signal intensity. Contrast enhancement is frequent and may be homogenous or heterogeneous.

Differential diagnosis is very challenging and includes metastatic carcinomas (most commonly of the lung), metastatic melanoma, and cardiac sarcomas. Angiosarcoma presents often similar localization (right heart) with pericardial effusion, but it can be more aggressive with malignant features such as evidence of hemorrhage and necrotic foci within the neoplasm. It also presents more intense and heterogeneous contrast-enhancement after contrast material administration on both CT and MRI [9].

Although CT and MRI provide high-resolution anatomic information, positron emission tomography/CT is a good method to distinguish between benign and malignant tumors adding information on the metabolic activity of lesions, gaining a key-role in the staging and follow-up of lymphomas (especially concerning more aggressive types with high glucose metabolism and Standardized Uptake Value such as diffuse B-cell non-Hodgkin lymphoma) [10].

However, final diagnosis is confirmed by pericardial fluid cytology and endomyocardial or excisional biopsy.

Prognosis in patients with PCL remains poor and late diagnosis seems to be the major cause affecting the outcome [6]. Surgical resection of PCL is often difficult and incomplete, and should be reserved for patients with life-threatening hemodynamic compromise [6,11]. Early systemic treatment appears to be the only chance for cure. Chemotherapy remains the preferred initial treatment, alone or in combination with radiation therapy [5,12].

References

- [1] Burke A, Virmani R. Tumors of the heart and great vessels. In: Atlas of tumor pathology. Washington: Armed Forces Institute of Pathology; 1996, p. 171–9.
- [2] Burke A, Jeudy Jr J, Virmani R. Cardiac tumours: an update. *Heart* 2008;94:117–23.
- [3] Gowda RM, Khan IA. Clinical perspectives of primary cardiac lymphoma. *Angiology* 2003;54:599–604.
- [4] Petrich A, Cho SI, Billett H. Primary cardiac lymphoma. *Cancer* 2011;117:581–9.
- [5] Nascimento AF, Winters GL, Pinkus GS. Primary cardiac lymphoma: clinical, histologic, immunophenotypic, and genotypic features of 5 cases of a rare disorder. *Am J Surg Pathol* 2007;31:1344–50.
- [6] Ceresoli GL, Ferreri AJM, Bucci E, Ripa C, Ponzoni M, Villa E. Primary cardiac lymphoma in immunocompetent patients: diagnostic and therapeutic management. *Cancer* 1997;80:1497–506.
- [7] Taylor AJ, Cequeira M, Hodgson JM, Mark D, Min J, O’Gara P, et al. ACCF/SCCT/ACR/AHA/ASE/ASNC/NASCI/SCAI/SCMR 2010 appropriate use criteria for cardiac computed tomography: a report of the American College of Cardiology Foundation Appropriate Use Criteria Task Force, the Society of Cardiovascular Computed Tomography, the American College of Radiology, the American Heart Association, the American Society of Echocardiography, the American Society of Nuclear Cardiology, the Society for Cardiovascular Angiography and Interventions, and the Society for Cardiovascular Magnetic Resonance. *J Am Coll Cardiol* 2010;56:1864–94.
- [8] Hundley WG, Bluemke DA, Finn JP, Flamm SD, Fogel MA, Friedrich MG, et al. ACCF/ACR/AHA/NASCI/SCMR 2010 expert consensus document on cardiovascular magnetic resonance: a report of the American College of Cardiology Foundation Task Force on Expert Consensus Documents. *J Am Coll Cardiol* 2010;55:2614–62.
- [9] Jeudy J, Kirsch J, Tavora F, Burke AP, Franks TJ, Mohammed TL, et al. From the radiologic pathology archives: cardiac lymphoma: radiologic/pathologic correlation. *Radiographics* 2012;32:1369–80.
- [10] Jhanwar YS, Straus DJ. The role of PET in lymphoma. *J Nucl Med* 2006;47:1326–34.
- [11] Fuzellier JF, Saade YA, Torossian PF, Baehrel B. Primary cardiac lymphoma: diagnosis and treatment. *Arch Mal Coeur Vaiss* 2005;98:875–80.
- [12] Ikeda H, Nakamura S, Nishimaki H, Masuda K, Takeo T, Kasai K, et al. Primary lymphoma of the heart: case report and literature review. *Pathol Int* 2004;54:187–95.